Photo-FETs: phototransistors enabled by 2D and 0D nanomaterials

Dominik Kufer[1] and Gerasimos Konstantatos[1,2,]*

[1]ICFO – Institut de Ciencies Fotoniques, The Barcelona Institute of Science and Technology, Castelldefels, 08860, Barcelona, Spain

[2]ICREA-Institució Catalana de Recerca i Estudis Avançats, Lluis Companys 23, 08010 Barcelona, Spain

E-mail: (Gerasimos.konstantatos@icfo.es)
Keywords: (photodetectors, quantum dots, 2D materials, photo-FET, phototransistors)

Abstract

The large diversity of applications in our daily lives that rely on photodetection technology requires photodetectors with distinct properties. The choice of an adequate photodetecting system depends on its application, where aspects such as spectral selectivity, speed and sensitivity play a critical role. High sensitivity photodetection covering a large spectral range from the UV to IR is dominated by photodiodes. To overcome existing limitations in sensitivity and cost of state-of-the-art systems, new device architectures and material systems are needed with low-cost fabrication and high performance. Low dimensional nanomaterials (0D, 1D, 2D) are promising candidates with many unique electrical and optical properties and additional functionalities such as flexibility and transparency. In this perspective, the physical mechanism of photo-FETs (Field Effect Transistors) is described and recent advances in the field of low-dimensional photo-FETs and hybrids thereof are discussed. Several requirements for the channel material are addressed in view of the photon absorption and carrier transport process, and a fundamental trade-off between them is pointed out for single-material based

devices. We further clarify how hybrid devices, consisting of an ultrathin channel sensitized with strongly absorbing semiconductors can circumvent these limitations and lead to a new generation of highly sensitive photodetectors. Recent advances in the development of sensitized low-dimensional photo-FETs are discussed and several promising future directions for their application in high sensitivity photodetection are proposed.

Photodetectors are one of the key components in many optoelectronic devices which transduce optical into electrical information. Today, photodetectors have reached a mature technology level and address a huge application spectrum including imaging, remote sensing, fibre-optic communication and spectroscopy among many others. However, to tackle challenges and to surpass existing limitations in sensitivity of state-of-the-art photodetector systems, new device architectures and material systems are needed which offer low-cost fabrication and high performance over a wide spectral range. The active research field on photodetection grows and many novel nanostructured material systems[1] have been employed for light sensing including Quantum dots[2,3], Perovskites[4,5], organic molecules and polymers[6,7], Carbon Nanotubes[8,9], Graphene[10,11] and the large field of semiconducting 2D materials such as the transition metal dichalcogenides (TMDCs) and black phosphorus[12,13].

Photodetector performance is governed by both the optical and electronic properties of the employed semiconductor. The former determines the spectral coverage and quantum efficiency of the detector whereas the latter determines, through the carrier transport and carrier density, the amount of dark current flowing through the device, as well as the efficiency of charge separation and collection upon illumination. The key parameters for a strong signal response are a high photon to electron conversion rate (quantum efficiency) and ideally an inherent gain

mechanism, which yields multiple carriers per absorbed photon. The response signal is then weighed against the noise portion of the ratio, which has to be minimized for maximum sensitivity. There are several device-external noise sources, such as the photon noise due to the statistical arrival of photons on the device or the read-out noise in photodetector arrays that originates in preamplifier electronics. Here, we will put emphasis on the device (photodetector pixel) inherent noise, which stems partially from thermally generated charge carriers and also from the intrinsic carrier density that contribute to the dark current of the device (shot noise limit) as well as flicker noise (1/f). It is however important to note that the sensitivity of a detector with inherent noise lower than the noise floor of commercially used CMOS read-out circuits, typically met in photodiodes, is limited by the latter, thus a photodetector technology with an inherent gain mechanism is desired to alleviate this effect.

The relevant performance metrics and terminology used throughout this article are described in Box 1.

Box 1 – Performance metrics for photodetection

Responsivity [A/W]

$$R = \frac{I_{Ph}}{P_{in}} = QE\ \frac{q\lambda}{hc}\ \frac{1}{\sqrt{1+(2\pi f\tau)^2}}\ G$$

Photocurrent	I_{Ph}
Incident light power	P_{in}
Quantum efficiency	QE
Electron charge	q
Incident wavelength	λ
Planck's constant	h
Speed of light	c
Modulation frequency	f
Time constant	τ
Photoconductive Gain	G

The fundamental process behind photodetection is absorption of light. Responsivity R, a measure of output current per incoming optical power in units of A/W, describes how a detector system responds to illumination. Responsivity depends on the incident wavelength, light modulation frequency and applied bias voltage. The response of a detector to light is primarily determined by the conversion efficiency of photon flux into electron flux, known as the

quantum efficiency (QE). The quantum efficiency typically takes into account all kind of external losses such as reflection and scattering and is often called external quantum efficiency (EQE). It is defined as the ratio of extracted electrons to incident photons, with a value between 0 and 100 %, unless carrier multiplication effects are present. In photodiodes the gain is equal to unity (G = 1) and charge extraction happens on extremely short time scales. The responsivity according to the equation above is then solely determined by the quantum efficiency. For instance, in the ideal case of 100 % conversion efficiency at a wavelength of 630 nm, the responsivity is 0.5 A/W.

Gain

$$G = \frac{\tau_{liftetime}}{\tau_{transit}} = \frac{\tau_{liftetime}}{L^2}\,\mu\,V_{DS}$$

Carrier lifetime	τ_{lifetime}
Carrier transit time	τ_{transit}
Channel length	L
Mobility	μ
Drain-source voltage	V_{DS}

In photoconducting systems a photoconductive gain mechanism can be present. In the most common case, one carrier type is trapped and the other is free to traverse the channel. If the trapping time, also referred to as lifetime, is longer than the transit time of free carriers, photoconductive gain is generated. This can lead to a large responsivity in orders of magnitude higher than for photodiodes. A similar effect is achieved in the case of imbalanced transport of electrons and holes (i.e. the mobility of one type of carriers differs than that of the other type). Photoconductors with large gain usually show rather slow response times as described by the so called gain-bandwidth trade-off. Since the response time constant and the photoconductive gain are dominated by the lifetime of trapped carriers, increasing gain decreases the operation bandwidth. This trade-off must be considered when designing detectors for specific applications.

Detectivity

[cm $Hz^{1/2}W^{-1}$= Jones]

$$D^* = \frac{\sqrt{A\,B}}{NEP} = \frac{R\,\sqrt{A * B}}{i_N}$$

Area	A
Bandwidth	B
Noise equivalent power	NEP
Responsivity	R
Noise current	i_N

The ultimate figure of merit to describe sensitivity of photodetectors includes both the response to light and the noise floor. The higher the signal-to-noise (SNR) ratio, the easier it is to detect the light signal. The lowest detectable power, when SNR = 1, defines the sensitivity limit of the detector and is called noise-equivalent power NEP. The noise equivalent power depends on many parameters that have to be taken into account and specified, such as detector area A, electrical bandwidth B and modulation frequency f. To facilitate the direct comparison between different detector architectures independent of area and bandwidth, a figure of merit named specific detectivity D* has been introduced. The detectivity still depends on certain

measurement conditions such as bias voltage, wavelength, temperature and modulation frequency, which have to be specified for comparison with other systems. State-of-the-art detectors such as silicon or InGaAs diodes demonstrate detectivities on the order of 10^{12} - 10^{13} Jones at room temperature.

Note: The noise current i_N comprises all noise sources present in a detector. The magnitude of noise at its operation frequency can be extracted from the spectral density of noise. Low-dimensional photo-FETs have been demonstrated to possess large flicker noise (1/f) components in the frequency range < 1kHz, at which they are usually operated. However, the detectivity is often stated in the shot-noise limit in which only the shot-noise current $I_{SN} = (2qI_{dark})^{1/2}$ is considered. The detectivity in the shot-noise limit can therefore overestimate the measured real detectivity by orders of magnitude in the discussed systems and careful attention is needed in the interpretation of the data. In addition to this, it should also be noted that once low dark current has been achieved and once the 1/f noise challenge has been addressed in these sytems, the Johnson noise will eventually take over determining the ultimate sensitivity of the device and thus should not be neglected in otherwise optimized detectors.

Photodiodes and photoconductors.

The two most common photodetector types are photodiodes and photoconductors. Photodiodes typically form a p-n-junction between oppositely doped semiconductors, a Schottky-junction between a doped semiconductor and one of the metal electrodes or one or more blocking contacts between intrinsic semiconductors or intrinsic semiconductors and metals (as in the case of polymer or perovskite based photodiodes) . The junction leads to charge carrier separation after the excitation process and electrons and holes drift in different directions towards the electrodes driven by the built-in electric field at the interface or by diffusion to selective contacts. The response time of diodes is determined by the transit time of carriers to their corresponding electrodes, leading to high-bandwidth operation in high carrier mobility semiconductors. The signal strength detected in diodes is dictated by the quantum efficiency. As charge carriers are separated by a built-in field at the junction, the device can at its best produce one electron-hole pair per absorbed photon, corresponding to a quantum efficiency of 100%. The potential barrier at the junction prohibits charge carrier recirculation and limits the response signal of photodiodes to unity gain. However, the SNR of photodiodes also benefits from the junction barrier as only few thermally generated carriers can cross the junction and

extremely low dark currents are achieved. The final limitation of sensitivity in this device configuration is likely to be given by external readout noise from preamplifiers. A particular class of photodiodes, the avalanche photodiodes (APDs) which are essentially photodiodes operated near the break down regime offer the possibility of extracting multiple carriers per single photon, similar to the concept of gain. Yet it has to be emphasized that this carrier multiplication effect present in APDs is qualitatively distinct than that of the gain in photoconductors. The carrier multiplication effect is due to quantum efficiency exceeding unity as the multiplication process takes place within the primary photocarrier generation. As a results APDs have the potential to reach simultaneously high responsivities at very bandwidth. The value of gain in APDs is typically on the order of 10-100 electrons per photon and requires the application of very high bias, typically exceeding 50-100 V. As a result the use of APDs is limited to metrology equipment where very high sensitivity and short time response is needed and the use of high bias and bulky electronics can be tolerated.

Photoconductors, on the other hand, can be operated at dark currents with noise levels beyond the read-out noise floor and have the potential to reach higher sensitivity than photodiodes. A photoconductor, in its most basic configuration, consists of a homogenous semiconductor slab with two ohmic metal contacts (drain D and source S). Photo-excited charge carriers are separated by an applied voltage V_{DS} and induce a change of carrier density which increases the devices` conductivity. In photoconductors the photoconductive gain can be present and is generated as soon as one photo-excited electron (hole) traverses the electrode spacing more than one time before recombination with a hole (electron). The most common reason for gain is trap-states (sensitizing centers) within the bandgap of the semiconductors, which capture and localize one charge carrier type and effectively prolong its carrier lifetime τ_{Lifetime}. The opposite carrier freely moves between source and drain driven by the applied electric field. The

photoconductive gain G is then defined as the ratio of lifetime and transit time (see Box 1). Photoconductors with large gain usually show orders of magnitude slower response times than diodes, because both the time constant and the gain are given by the lifetime of the trapped carriers. However, they have the potential for extremely high sensitivity due to the gain mechanism. Ideal conditions for gain are met in high mobility semiconductors with high quality ohmic contacts, since Schottky-barriers at the contacts can strongly impede efficient charge replenishment and reduce photoconductive gain. Ohmic contacts, however, also imply large dark currents and therefore large photoconductive gain does not necessarily lead to higher SNR, as it is often assumed. While the SNR of a detector pixel with gain is maintained rather constant due to simultaneous amplification of signal and noise, the real benefit of gain is to raise the signal above the noise floor of the readout system to avoid performance limitations by the signal processing electronics. An optimized point of gain-operation has to be found, since the high dark currents of devices with extremely large gain lead to other fundamental drawbacks such as high power consumption. Additionally it adds on the complexity of the signal read-out process as large dark currents saturate read-out electronics[6], calling for design of complex read-out schemes.

Another class of photodiodes has been introduced recently which can be considered as a hybrid photodiode-photoconductor systems [Jinsong Huang]. In that case photogenerated carrier trapping at an interface (typically a Schottky junction) transforms, upon illumination, a rectifying contact into an ohmic contact, henceforth transforming the detector from a photodiode in dark into a photoconductor under illumination.

Photo-FETs.

A promising device architecture that can concomitantly achieve low dark current and high gain is the photo field-effect transistor (photo-FETs). As illustrated in **Figure 1**, the device

configuration is similar to lateral photoconductors with metal-semiconductor-metal architecture forming the source and drain electrodes. Yet a third contact, the gate electrode which is electrically isolated from the semiconductor channel by a thin dielectric film can be exploited to modulate the conductivity of the channel. An applied gate voltage V_{GS} can be used to control electronically the carrier density by field-effect modulation and favourably switch off the dark current by operating the device in the depletion regime. The incident light activates the channel conductance of the device, through carrier photogeneration, which then ideally profits from a photoconductive gain mechanism as in photoconductors. For high performance photo-FETs, the channel material should ideally possess high carrier mobility for high gain-bandwidth products, a moderately large and direct bandgap for efficient field-effect modulation and optical absorption, and a thin profile for full depletion and operation at ultralow dark currents. Moreover the channel material should exhibit very low trap state density to yield low sub-threshold swings.

Especially the group of 2D layered materials fulfil most of these requirements. The discovery of graphene led initially to extensive studies on its own use for photodetection[14–20], due to excellent charge carrier mobilities, broadband absorption, and mechanical flexibility. However, the lack of bandgap in graphene and its corresponding large dark currents remain one of the main challenges if operated in photo-FET configuration and demand special read-out schemes in order to exploit the full potential of this material platform.

Researchers soon expanded into other 2D materials[21], which share similar properties like the atomic thickness and flexibility, but also complement graphene with further functionalities[22]. The group of semiconducting transition metal dichalcogenides (TMDCs) emerged as a promising candidate for both conventional semiconductor technology and flexible technology in view of its ultimate scalability down to the atomic level and the presence of bandgap. With

decreasing layer thicknesses, quantum confinement effects come into play, leading to a sizeable optical absorption edge between 1-2eV that is highly interesting for photodetection. Photo-FETs based on plain MoS_2[23–33], WSe_2[34], $MoSe_2$[35–37] and WS_2[38–40] consisting of single- and multilayer nanosheets have been demonstrated. While sensitivity is limited to the visible for monolayers due to the direct bandgap, the bandgap turns indirect and shrinks with increasing layer number extending thereby detector sensitivity into the NIR region. Apart from the TMDCs many more layered material systems have been explored in photo-FET device configuration with similar performance, including other chalcogen-based materials such as GaS, GaSe, GaTe, SnS_2, InSe, In_2Se_3[41–48] and the recently discovered black phosphorus[41,49,50]. Few-layer black phosphorus emerged as highly promising candidate with highest mobility reported of 1000 cm^2/Vs and a thickness dependent bandgap from 0.3-2.0 eV[51], an attractive spectral range that cannot be fully reached by TMDCs, yet its environmental stability remains a concern for robust devices.

Molybdenum disulfide is one of the most studied semiconducting layered materials of all the aforementioned, due to the natural occurrence of MoS_2 single crystals and its high performance on commonly used Si/SiO_2 substrates contacted with standard contact metals. Monolayer MoS_2 photodetectors are especially promising for flexible and semitransparent device concepts due to its mechanical flexibility and strength[52–55]. One of the most intriguing properties of monolayer MoS_2 is its large direct bandgap of 1.8eV, which leads to high absorption efficiency[56,57] and large electrical on/off ratios. Experimentally on/off ratios of 10^8 have been reported[58,59], with theoretical predictions[60] even reaching 10^{10}. The gate-tunable conductivity allows to fully deplete the MoS_2 channel and due to the atomically thin profile of monolayer MoS_2 extremely low off-current densities of 25fA/µm have been achieved to date[59]. This means that MoS_2 photo-FETs with dimensions of 1um x 1um can already reach dark currents of only

1 order of magnitude higher than commercial, uncooled InGaAs photodiodes with the same dimensions.

The optoelectronic response to light of monolayer and few-layer 2D semiconductors has shown an enormous variety in performance parameters, reporting responsivity from 10^{-3}-10^{3} A/W and temporal response times in the range of 10^{-5}-10s.[12,13] A prominent reason for that was found to be the large surface-to-volume ratio of 2D materials. Diverse substrate treatments prior to MoS_2 deposition have shown to strongly impact responsivity and response time by introducing trap states in the bandgap, which capture holes and increase their lifetimes leading to responsivity of 880A/W and decay times of 9s and longer[23]. Furchi et al. have shown that the photoresponse of MoS_2 is based on two distinct mechanisms, the photogating and photoconducting effect[30]. The photogating mechanism originates from long-lived charge-trapping processes at surface-bound water molecules or other surface adsorbates and is responsible for the extremely slow response dynamics and high responsivity values. The photoconducting mechanism has been demonstrated by applying two light sources, where a continuous light source fills adsorbate-related traps and a rapidly modulated light source probes the material-related photoconductivity. Under these conditions much lower optical gain and fast response times are observed. An important step to successfully employ 2D materials as ultra-thin photodetectors is therefore to control the impact of substrate and surrounding atmospheric adsorbates, to achieve high sensitivity together with fast response times. A robust passivation scheme has recently been proposed by encapsulating MoS_2 photo-FETs with atomic layer deposited (ALD) oxides[58] such as HfO_2 and Al_2O_3. The isolation from ambient air enhanced electronic properties and led to experimentally measured sensitivity of 10^{11} - 10^{12} Jones with decay times of 10 ms. The responsivity and temporal response could be tuned by field effect modulation by orders of magnitude with R = 10 – 10^4 A/W and corresponding time response of t = 10ms to 10s. The large responsivity of 10^4 A/W due to strong signal amplification was obtained in the

accumulation regime of the photo-FET, in which also highest dark currents are reached and the sensitivity of the detector dropped to its minimum. The large variety of reported performance parameters can be attributed to different environmental measurement conditions, different substrate treatments and optoelectronic characterisation under different backgate field strength.

Trade-offs in low-dimensional photo-FETs.

In photo-FETs based on single semiconductor channels such as plain TMDCs a trade-off is found, because both the absorption and the amplification process appear within the same channel. This dilemma is described in **Figure 2**. The two left columns depict the example of an extremely thin channel with thickness t_{ch} in the few-nanometer range compared to a rather bulky channel with t_{ch} in the range of a few hundred nanometer. Both show modulation curves as typically found for n-type semiconductors. While the thin channel reaches large on/off ratio and can be electrically operated in full depletion, the bulky channel suffers from largely reduced on/off ratio as the channel cannot be switched off entirely. The field-effect capacitive coupling mostly affects the lower part of the thick semiconductor and a significant amount of leakage current can still traverse trough the upper part of the channel increasing the dark current. The absolute optical absorption on the other hand is more efficient for thicker channel due to the longer optical absorption path of photons through the material slab.

Another trade-off, which is inherent to many 2D layered semiconductors, is the thickness dependent spectral coverage. The thinnest channel possess the largest bandgap for these material family and are in favour for high electrical on/off ratios and operation at low dark currents. However, the large bandgap limits its absorption properties in the UV-visible part of spectrum.

Apart from the low absolute absorption in ultra-thin channels, there are other mechanisms inherent to 2D materials like MoS_2 that lead to recombination losses. Due to spatial

confinement in the z-direction and low electrostatic screening[62], electron-hole pairs are strongly bound to each other, with reported exciton binding energies of 300-900 meV [63–66], far beyond the room temperature thermal energy of 25meV. Impractically high electric fields are needed to efficiently separate photogenerated excitons which easily recombine. Strong coulomb interactions in 2D materials have been shown to favour Auger scattering processes, which lead to capture of electrons and holes at defect sites and eventually high recombination rates resulting in poor quantum efficiencies of MoS_2 optoelectronic devices[67].

The quantum efficiency of reported monolayer MoS_2 photo-FETs can roughly be calculated from the measured responsivity and from an estimation of the photoconductive gain (Box 1). While the measured exponential decay time corresponds to the lifetime of photo-excited carriers, the transit time can be determined knowing the channel length, applied bias, and mobility. This simple estimation leads to rather poor quantum efficiencies of 0.0002 - 0.02%[23,26,58,67] and indicates a significant amount of recombination losses before the charge carriers can be extracted into the electronic circuit. It is noteworthy that a high density of shallow trap states within the bandgap can cause longer observed decay times than the actual lifetime of free carriers[68]. In that case, the above estimated quantum efficiency is underestimated and states a lower limit.

This trade-off is a common issue for low-dimensional photodetectors and needs a new perspective for enhanced light-matter interaction. Next to plasmonics[62] and optical cavities[69] for enhanced absorption, another very encouraging method is to sensitize a thin channel material with strongly absorbing semiconductors (sensitizers) of opposite doping polarity to create a vertical heterojunction (**Figure 2**, right column). The decoupling of the absorption process (in the sensitizer) from the charge transport (in the channel), allows operation of the thin channel in full depletion while the sensitizer provides high absorption, ideally without

interfering the electrical modulation. The thickness of the decorating sensitizer can be in dimensions similar to the discussed bulk case of a thick plain channel and thereby transport and absorption properties are similarly optimized. The built-in field at the junction plays a critical role in this novel device concept for efficient exciton separation and charge injection into the channel, as will be explained in more detail later. Its formation can be recognized by a vertical shift of the modulation curve $I_{DS} - V_G$ under dark conditions due to the charge flow until the alignment of Fermi levels to equilibrium (see **Figure 2** – right column).

The device schematic in **Figure 3** displays the working principle of a sensitized photo-FET, using the example of a 2D material channel decorated with colloidal QDs. After the absorption process, a fast recombination of photogenerated carriers is prevented due to spatial separation of carriers in the heterojunction. The p-n-junction between the oppositely doped semiconductors leads to a vertical photodoping effect and the injected electrons (holes) are transported laterally through the channel. As long as the holes (electrons) maintain trapped within the sensitizer, the electrons (holes) can recirculate the channel and generate gain.

Despite the missing bandgap, graphene is an interesting candidate to form hybrid sensitized phototransistors, mainly due to its unprecedented high mobility and sensitivity to electrostatic perturbation by photo-excited charge carriers in its vicinity[10]. The high carrier mobility is promising for device concepts with large carrier multiplication and extremely high gain-bandwidth products. Several sensitizers have been implemented including QDs[70,71], Perovskites[72], CNTs[73] and even other 2D materials such as MoS_2[74–76]. The most sensitive graphene-based hybrid detector has been reported for a graphene/PbS QD combination. The ultrahigh gain of 10^7 electrons per photon has led to a detectivity beyond 10^{13} Jones, despite the large dark currents present in graphene[70].

The growing amount of discovered semiconducting layered materials with large bandgaps and high in-plane mobility may even lead to higher performance in terms of sensitivity. Sensitive photo-FETs have been demonstrated by applying a similar approach employing a MoS_2 channel decorated with PbS QDs[61]. The spectral response of plain MoS_2, covering solely the visible spectral range, was thereby increased to NIR/SWIR due to the tunable absorption spectra of colloidal quantum dots. The responsivity improved by several orders of magnitude over its single counterparts and reached values of 10^5-10^6A/W due to large carrier multiplication. However, the tremendous improvement in responsivity came with the loss of its initially high gate-tunable on/off ratios, the major strength of TMDCs to reach low off-currents. A high density of interface traps was found to be the reason for the loss of gate-control, which could be prevented by selective interface engineering of the MoS_2/PbS interface[77]. A passivating TiO_2 buffer layer has been implemented to preserve control of field-effect modulated dark current and to strongly reduce noise. The device sensitivity and response time were thereby enhanced by more than an order of magnitude to an experimentally determined D* of $5*10^{12}$ Jones and 12 ms, respectively. In the shot-noise limit these devices can reach detectivities beyond 10^{14} Jones showcasing the immense potential of this device concept with further reduction of noise (mainly 1/f noise). An estimation of quantum efficiency based on the ratio of decay and transit time leads to considerable improvement over plain MoS_2 photo-FETs with values up to 28%. Compared to the aforementioned graphene phototransistors, the MoS_2/TiO_2/PbS hybrid could be operated at dark currents of more than 5 orders of magnitude lower than typically reached in graphene devices.

The concept of sensitized high mobility materials does not only apply to 2D layered materials. A hybrid photo-FET based on PbS QD/indium gallium zinc oxide (IGZO) has been developed[78]. The amorphous metal oxide semiconductor IGZO is a novel material with promise for low-cost and large-area thin film transistor technology[79]. Its application as a photo-FET

channel material enabled a highly sensitive hybrid photodetector with excellent photoresponsivity of 10^6A/W and detectivity of 10^{13} Jones in the NIR. Next to graphene also other carbon-based nanomaterials such as carbon nanotubes (CNTs) have been extensively studied for photodetection[8,9]. CNTs possess similarly large mobility from 10^2-10^4 cm^2/Vs depending on fabrication method and the additional benefit of a bandgap for gate modulation with on/off ratios ranging from 10^3-10^6.[80–82] Although its electrical properties are excellent for charge transport, the inefficient absorption within the one-dimensional body calls for a sensitizing approach. Light induced charge transfer, increased photosensitivity, and reported responsivities up to 10^2 – 10^4A/W have been achieved by combining CNTs with quantum dots[83–85], perovskites[86], polymers and molecules[87–90], and fullerene (C_{60})[91]. In some of these device concepts the sensitizer is used for enhanced absorption and carrier injection of photoexcited charge carriers into the CNTs which serves as the transport medium. In others, the sensitizer is simply applied as a carrier acceptor to enhance the exciton dissociation in CNTs and to overcome the obstacle of fast recombination events due to the large exciton binding energies.

Backgate dependent performance metrics.

A major advantage of the sensitizing technique over single material photo-FETs is that the size of the channel bandgap can be arbitrary and it can be either direct or indirect as the absorption process is now outsourced to the sensitizer. It is consequently profitable to employ large bandgap materials for the transport channel to achieve large on/off ratios and low dark current in the depletion regime. Moreover, the channel material should provide high carrier mobility to obtain short transit times and to produce moderate photoconductive gain together with fast response times.

In **Figure 3,** two transfer curves of sensitized photo-FETs with a n-type semiconductor channel and a p-type sensitizer are compared in the real and the theoretically ideal case. Both devices are considered to be fabricated on the same substrate with equally thick dielectric oxide. Upon light illumination, the curves shift to the left indicating a n-type doping effect by electron injection from the sensitizer into the channel. If operated in its depletion regime ($V_G < V_{Th}$), the hybrid device shows lowest dark currents but also smallest photocurrents I_{Ph}. If operated in the accumulation regime ($V_G > V_{Th}$), the device exhibits extremely large dark currents but also higher photocurrents due to higher current amplification (gain). The ideal point of operation, named as most sensitive point $V_{MSP,}$ is located somewhere in between, close to the current onset of the characteristic transfer curve where the photo-FET operates at highest SNR. Comparing the real with the ideal case, it is obvious that significant improvement of device performance in terms of gain can be achieved for FET devices with faster switching from off- to on-states, leading to higher current amplification. Apart from high carrier mobility, which increases the slope of the transfer curve and thereby the photoconductive gain, ideal off-state conditions, i.e. a low inverse sub-threshold slope $S = d(V_{GS})/ d(\log(I_{DS}))$, can largely improve photo-FET performance. Several studies on transport mechanisms of FETs based on CNTs[92–94], ultrathin Si MOSFETs [95], MoS_2[96] and black phosphorus[97] have demonstrated that the appearance of significant Schottky barriers (SB) at the metal semiconductor interface in these systems lead to decreased switching speed with subthreshold slopes far beyond the ideal 60meV/dec at room temperature. Unlike conventional Si MOSFETs, the gate voltage also modulates the SB at the contact and apart from thermionic emission a considerable tunnelling component is responsible for the current flow through the channel. To improve characteristic FET properties it is desirable to minimize the SB height and width to maximize the tunnelling probability. The detrimental impact of large Schottky barriers is one of the major remaining obstacles for FETs based on low-dimensional materials such as TMDCs. For better photo-FET performance it will

therefore be a critical step to achieve high contact quality, as it will not only improve gain but also impacts on noise operation [98].

For few-layer TMDC FETs an improvement of contact resistance, subthreshold swing, and efficient charge injection has been demonstrated in different ways; (i) the choice of an appropriate metal contact which forms the lowest SB despite the occurring fermi level pinning effects. Encouraging results were reported for low work function metals[96,99] and gate tunable graphene edge contacts[100]. (ii) A high degree of doping in the contact region of the channel to promote strong band bending at the metal-semiconductor interface and to make the SB thinner and therefore more transparent [101–103]. (iii) The decrease of defect and trap density, caused by sulphur vacancies or the semiconductor/dielectric interface, improves the subthreshold swing due to a faster transition from the insulating regime, where E_F lies within the bandgap, to the conducting transport regime, where E_F lies inside the conduction band. The large amount of localized states next to the conduction band edge leads to a gradual transition from the one to the other. The conduction process in the region of localized states is based on variable range hopping (VRH)[104–106] and thermally activated transport, whereas band-like transport dominates at higher carrier densities[107]. It was shown for MoS_2 that a decrease in defect density can lead to shorter subthreshold swings[63,108] and therefore a faster transition from off- to on-state. (iv) By operating the device at lower temperatures far superior mobility compared to room temperature operation have been demonstrated due to decrease of phonon-scattering and effective screening of charged impurities[100,104,109].

All the aforementioned options are promising to further enhance effective transport of photogenerated carriers through the channel in sensitized hybrid photo-FETs. It is noteworthy that the use of thinner high k-dielectrics between gate electrode and channel can strongly decrease the subthreshold swing of SB-FETs[92], but will not improve the optical photoresponse of the device. It instead results in stronger capacitive coupling between gate and source-SB and

allows electrically similar I_{DS} switching by tuning through a smaller interval of backgate voltage. An improvement of photo-FET performance can however be expected for faster switching devices if the same dielectric film thickness is considered.

Apart from dark current and gain, also the quantum efficiency of hybrid photo-FETs is dependent on the field-effect modulation via backgate. The coloured boxes on the right of **Figure 3** depict the band alignment of three different regimes of operation. Exciton separation and charge injection into the channel is determined by the band alignment of the two semiconductors in contact, which in turn is strongly dependent on the gate-tunable Fermi level E_F. Ideally the sensitizer is electrically isolated from source-drain contacts to be unaffected by the gating (constant position of E_F in the p-type sensitizer) and to not attribute to leakage current when the channel is in off-state operation. The best condition is then given in the accumulation regime, where E_F approaches the conduction band. In this case, the high electron density of the channel induces the largest depletion region within the hole-doped sensitizer. The least favorable condition is given in the depletion regime, where the channel turns rather intrinsic and the band bending at the interface reaches its minimum. The optimized point of the overall photo-FET operation will again be somewhere in between, here named as “operational” regime, where the best performance between dark current, gain and quantum efficiency has to be identified.

Ideal sensitizer characteristics.

In principle any absorbing material can serve as a sensitizer for the device concept of hybrid photo-FETs: semiconductors can serve as strong absorber in which the bandgap curtails spectral selectivity, semimetals such as graphene can be used as constant broadband absorber over a large spectral range, and even metallic nanostructures can be employed as resonant

plasmonic absorber. The latter, however, have to rely on a different mechanism of sensitization so as not to compete with the very fast recombination present in metal and semimetals. This can be achieved by employing bolometric detection by altering the local temperature and therefore the conductance of the channel or by photothermionic injection of hot carriers generated in plasmonic metallic or graphene nanostructures atop a semiconducting layered channel. However, for an optimized performance, the sensitizer should fulfil certain requirements: (1) The doping polarity of a doped absorbing material is opposite to the channel material to achieve large built-in fields for efficient charge carrier separation and vertical injection into the channel. Alternatively the sensitizing material can also be intrinsic (i.e. have very low intrinsic carrier density) provided it forms a type-II hterojunction with the 2D channel and possess long carrier diffusion lengths to facilitate charge collection in the 2D channel in the absence of a built-in electric field. (2) The sensitizer has a low exciton binding energy and long lifetimes, which is reflected in long carrier diffusion length of several hundred nanometers. This allows to increase the thickness of the absorber to achieve strong absorption in absolute terms, but also to maintain high injection rates into the underlying channel. Here, one has to differentiate between two extreme cases, the fully depleted thickness t_{depleted} and the saturated thickness $t_{\text{saturated}}$, between which the optimized thickness of the sensitizing film has to be found. The thickness t_{depleted} refers to a fully depleted, thin absorbing layer for which charge carrier injection is dominated by drift induced through the built-in field. In the case of $t_{\text{saturated}}$ the film reached a thickness beyond the diffusion length of the photogenerated excitons and recombination losses start to decrease the photoresponse of the hybrid. In the case of materials with high exciton binding energies such as in the case of polymers, the employment of a bulk heterojunction is required, similar to photovoltaic architecures, in order to dissociate excitons within the bulk of the absorber into free charges that will subsequently diffuse to the 2D channel provided a thermodynamically favoured band alignment (type II) (3) The

absorbing film has to be readily integrated with the FET channel and is ideally compatible with standard CMOS technology or even mechanically flexible device concepts. Solution-processed materials hold therefore a general advantage for they can easily be spin- or spray-coated on top of any substrate and FET-device without requirements such as lattice mismatch. (4) A high absorption coefficient with large spectral coverage and tunability over a wide wavelength range adds a major advantage to sensitized photo-FETs over simple single channel devices. The absorption is now taking place in the decorating film and adds therefore another degree of freedom to device design and application.

Colloidal quantum dots have well matched properties to fulfil most of the requirements. In the case of widely used PbS, the most intriguing characteristic for photodetection is the tunable bandgap due to the quantum confinement effect[110]. By simply changing the size of QDs during synthesis, the exciton peak can be shifted through a large spectral range from 500 – 2100nm[111–113]. The low exciton binding energy[114] and the diffusion length of 150-250nm[115] suggest an electrically ideal sensitizer to reach high optical absorption and high quantum efficiency. A wide range of doping strategies have shown both doping polarities in PbS QDs[116], making it a versatile sensitizing system to combine with any channel material. Solution-processed CQD optoelectronic devices have already demonstrated compatibility with CMOS technology[117,118] and flexible device concepts[119,120].

Another emerging solution-processed material with promise for optoelectronic applications such as solar cells is the family of inorganic-organic perovskites[121]. Rapid advances in this young research field has led to spectral tunability from 400-800nm[122] and extremely large exciton diffusion length of around 1µm for polycrystalline thin films[123]. Organolead trihalide perovskite single crystals have been reported by implementing a novel antisolvent vapour-assisted growth technique. The single crystalline structure exhibits trap state densities as low

as 10^9 per cubic centimetre and reached remarkable diffusion length of more than 10 µm [124]. Several types of photodetectors based on photoconductors, photodiodes and phototransistors with broadband absorption[125–129] and tunable narrowband absorption[5, 130] in the visible have been demonstrated, both being interesting features for sensitized photo-FETs.

Future outlook on sensitized photo-FETs

To date, many prototype devices have shown promising outcome, however there is still plenty of space for further improvement on all performance parameters. Several aspects such as the huge variety of materials for channel and sensitizer or the additional implementation of other compounds at the bottom (substrate treatment), the interface or on top of the device, open new opportunities to develop novel photo-FET architectures with sensitivity superior to existing photodetection technology. In the following, we summarize a few ideas and device concepts which give the direction to a new generation of photo-FETs.

The major strength of 2D material phototransistors is the high in-plane charge carrier mobility and potentially low dark current given by its thin channel body and efficient capacitive control over carrier density by means of the electric field effect. The choice of channel material will therefore play a critical role for further development. Reported mobilities for commonly investigated 2D materials are widespread and, so far, a trade-off is met between reported mobility and bandgap[131,132], which in turn determines the on/off ratio. Two popular examples are graphene, with average mobilities of 10^4 cm^2/Vs and on/off ratios of 10, and MoS_2, with mobilities of 1-80 cm^2/Vs and on/off ratios of 10^8.[133] An interesting candidate between these two extreme cases is black phosphorus. The combination of on/off ratios of 10^4-10^5 and mobility up to 1000cm^2/Vs[51,134]is intriguing for its application in hybrid phototransistors to achieve high gain-bandwidth products and sufficiently low off currents for high sensitivity detection.

Most of the prototype devices have been demonstrated with channel area far beyond $1um^2$. For high pixel integration in photodetector arrays, the successful development of well performing hybrid photo-FETs with a footprint below $1um^2$ is highly interesting. A benefit of decrease in channel length would be the shortening of carrier transit times. Consequently, careful trap state engineering in the sensitizer could be employed to introduce rather shallow trap states and likewise decrease the lifetime of photogenerated carriers. While the photoconductive gain would thereby largely be unaffected, the rather slow response times reported to date in the range of 10ms to 1s could be further improved. Despite the favourable prediction of device shrinking for gain, the impact of electrode contacts on noise remains an interesting open question. The smaller the channel length the more dominating the impact of contact noise will be. At the same time though real-world applications would require the fabrication of millions of small pixels into large arrays ideally employing wafer scale processing. Thus apart from addressing the miniaturization challenge of the single pixels an even greater challenge emerges in growing large area high quality and high uniformity 2D materials using high throughput manufacturing processes and with electronic properties at least on par with those attained on exfoliated 2D flakes.

An important device parameter to optimize is the quantum efficiency of hybrid photo-FETs. A key role can there be attributed to the interface of channel and sensitizer, as the photocarrier separation and charge injection into the channel take place in this region. The integration of a buffer layer at the interface of a MoS_2/PbS photodetector has shown to strongly impact on electrical tunability due to controlled doping and defect passivation[77]. Apart from ALD-deposited thin films employed in this study, the exploitation of molecular self-assembled monolayers at the interface may also lead to efficient crosslinking between QDs and TMDCs and simultaneously passivate electronic defect states at the TMDC surface as demonstrated for other materials in solar cell devices[135–137].

Towards the goal of even higher quantum efficiency of QD-sensitized channels, knowledge from advances made in intensively studied solar cell junctions can be helpful. For instance, the usage of different capping ligands for several QD layers can engineer the band alignment in a way to extend the depletion width within the QD film[138]. A cascade-like alignment of the conduction band would thereby improve the electron transfer towards the channel-QD junction and increase the charge collection efficiency, allowing thicker QD films with higher absorption.

A different approach with better control of charge carrier injection from the sensitizer into the channel is the incorporation of a transparent electrode on top of the sensitizing film, as shown for graphene/PbS hybrid detectors[139]. With the top electrode acting as a cathode and the graphene channel as acceptor contact, charge carriers can be efficiently directed towards the channel relying on bias controllable carrier drift rather than diffusion processes. An improvement of quantum efficiency to a value of approximately 80% along with significant improvement in device speed and dynamic range has been demonstrated. This was achieved by essentially transforming the sensitizing quantum dot layer into an active photodiode. This not only led to record quantum efficiency but acts as a paradigm shift in photo-FETs. The gain in this architecture is determined by the ratio of the transit time of minority carriers in the QD film over the transit time of majority carriers in the channel. This thus opens the way towards high gain and high bandwidth detectors tailored by the carrier mobilities of the channel and the sensitizing layer.

The versatile incorporation of any solution-processed material is one of the strongest features of this hybrid detector design. Hybrid systems using QDs have already shown sensitivity on par with detector technology based on silicon and InGaAs for the vis-SWIR range and have the potential to clearly outperform their sensitivity. In the MIR wavelength regime, for instance, conventional technology is made of epitaxial InSb and HgCdTe, which are extremely

expensive and require cooling for high performance[140]. The synergy of 2D materials with MIR-sensitive QDs, such as HgTe, therefore constitutes a compelling alternative to epitaxially grown state-of-the-art detectors and deserves investigation also towards the discovery of MIR-sensitizers comprising environmentally friendly elements and offering significant robustness to oxygen and moisture.

In general, the sensitizing material does not necessarily have to be solution-processed. The use of thicker slabs of layered 2D materials as sensitizer on top of ultrathin 2D material channels for transport may form interesting photo-FET hybrids. A large bandgap material like monolayer MoS_2 for charge transport decorated with an electrically isolated, narrow bandgap material like multilayer black phosphorus could strongly profit from a clean interface structure with efficient charge injection and low noise operation. The progress in CVD based large-scale film growth and the direct growth of heterostructures can play a key role for the development of novel photo-FETs based on all-layered materials.

The development of photo-FETs with strongly reduced dark currents and moderate gain does not exclusively rely on the decoupling of absorption and transport in two different semiconducting media. Adinolfi *et al.* have demonstrated a junction field effect transistor (JFET), in which photon absorption and charge transport occur within a PbS QD film[141]. By adding electrically isolated molybdenum trioxide (MoO_3) on top of the film, the formed rectifying junction between deep work function MoO3 and PbS provided full depletion and strongly reduced currents under dark conditions. The photo JFET operated with moderate gain of 10 at considerably high modulation frequencies of up to 100 kHz. Ma *et al.* reported similarly on $WS_2/CH_3NH_3PbI_3$ heterostructures where the TMDC layer led to suppression of dark currents compared to plain perovskite control devices[142]. Here, both components are electrically active and transport carriers between drain and source contacts. A favourable band

alignment enhanced the photocarrier separation at the TMDC/perovskite interface and improved the overall signal-to-noise ratio with reported specific detectivity of 10^{12} Jones.

Conclusions.

In optoelectronic technology, photodetectors are of paramount importance, and the growing diversity of applications demands new material systems and device designs. In this review, we have shown that photo-FETs based on low-dimensional materials are a highly promising novel device concept for high sensitivity photodetection. The gate controllable low dark current and photoconductive gain provide with excellent signal-to-noise ratios, specifically important for low light detection. We have discussed an inherent trade-off in plain low-dimensional photo FETs between transport and absorption processes, and proposed a solution by decoupling the absorption from transport with a sensitizing approach. For many different types of low dimensional materials (0D, 1D and 2D), the sensitizing to hybrid photo-FETs has proven to outperform their single counterparts in terms of sensitivity and indicates the abundance of nanomaterial combinations within this device concept. At this point, we have only seen some reports on proof-of-principle devices, but there is no doubt that the concept of hybrid photo-FETs has a lot to offer to the photodetection community and future technology.

Acknowledgments:

We acknowledge funding from Fundació Privada Cellex, and European Commission's Seventh Framework Programme under Graphene Flagship (contract no. CNECT-ICT-604391). We also acknowledge financial support from the Spanish Ministry of Economy and Competitiveness (MINECO) and the "Fondo Europeo de Desarrollo Regional" (FEDER) through grant MAT2014-56210-R. This work was also supported by AGAUR under the SGR grant (2014SGR1548). G.K. acknowledges financial support from the Spanish Ministry of Economy and Competitiveness, through the "Severo Ochoa" Programme for Centres of Excellence in R&D (SEV-2015-0522). D.K. is supported by an FI fellowship.

References

(1) Chen, H.; Liu, H.; Zhang, Z.; Hu, K.; Fang, X. Nanostructured Photodetectors: From Ultraviolet to Terahertz. *Adv. Mater.* **2016**, *28*, 403–433.

(2) Saran, R.; Curry, R. J. Lead sulphide nanocrystal photodetector technologies. *Nat. Photonics* **2016**, *10*, 81–92.

(3) Konstantatos, G.; Sargent, E. H. Solution-Processed Quantum Dot Photodetectors. *Proc. IEEE* **2009**, *97*, 1666–1683.

(4) Docampo, P.; Bein, T. A Long-Term View on Perovskite Optoelectronics. *Acc. Chem. Res.* **2016**, *49*, 339–346.

(5) **Lin, Q.; Armin, A.; Burn, P.L.; Meredith, P. Filterless narrowband visible photodetectors.** ***Nat. Photonics*** 2015**, *9*, 687-694.**.

(6) Baeg, K.-J.; Binda, M.; Natali, D.; Caironi, M.; Noh, Y.-Y. Organic Light Detectors: Photodiodes and Phototransistors. *Adv. Mater.* **2013**, *25*, 4267–4295.

(7) Jansen-van Vuuren, R. D.; Armin, A.; Pandey, A. K.; Burn, P. L.; Meredith, P. Organic Photodiodes: The Future of Full Color Detection and Image Sensing. *Adv. Mater.* **2016,** doi:10.1002/adma.201505405.

(8) Avouris, P.; Freitag, M.; Perebeinos, V. Carbon-nanotube photonics and optoelectronics. *Nat. Photonics* **2008**, *2*, 341–350.

(9) He, X.; Léonard, F.; Kono, J. Uncooled Carbon Nanotube Photodetectors. *Adv. Opt. Mater.* **2015**, *3*, 989–1011.

(10) Koppens, F. H. L.; Mueller, T.; Avouris, P.; Ferrari, A. C.; Vitiello, M. S.; Polini, M. Photodetectors based on graphene, other two-dimensional materials and hybrid systems. *Nat. Nanotechnol.* **2014**, *9*, 780–793.

(11) Sun, Z.; Chang, H. Graphene and Graphene-like Two-Dimensional Materials in Photodetection: Mechanisms and Methodology. *ACS Nano* **2014**, *8*, 4133–4156.

(12) Buscema, M.; Island, J. O.; Groenendijk, D. J.; Blanter, S. I.; Steele, G. A.; van der Zant, H. S. J.; Castellanos-Gomez, A. Photocurrent generation with two-dimensional van der Waals semiconductor. *Chem. Soc. Rev.* **2015**, 44, 3691-3718

(13) Pospischil, A.; Mueller, T. Optoelectronic Devices Based on Atomically Thin Transition Metal Dichalcogenides. *Appl. Sci.* **2016**, *6*, 78.

(14) Park, J.; Ahn, Y. H.; Ruiz-Vargas, C. Imaging of Photocurrent Generation and Collection in Single-Layer Graphene. *Nano Lett.* **2009**, *9*, 1742–1746.

(15) Lee, E. J. H.; Balasubramanian, K.; Weitz, R. T.; Burghard, M.; Kern, K. Contact and edge effects in graphene device. *Nat. Nanotechnol.* **2008**, *3*, 486–490.

(16) Xia, F.; Mueller, T.; Golizadeh-Mojarad, R.; Freitag, M.; Lin, Y.; Tsang, J.; Perebeinos, V.; Avouris, P. Photocurrent Imaging and Efficient Photon Detection in a Graphene Transistor. *Nano Lett.* **2009**, *9*, 1039–1044.

(17) Mueller, T.; Xia, F.; Avouris, P. Graphene photodetectors for high-speed optical communications. *Nat. Photonics* **2010**, *4*, 297–301.

(18) Pospischil, A.; Humer, M.; Furchi, M. M.; Bachmann, D.; Guider, R.; Fromherz, T.; Mueller, T. CMOS-compatible graphene photodetector covering all optical communication bands. *Nat. Photonics* **2013**, *7*, 892–896.

(19) Xia, F.; Mueller, T.; Lin, Y.-M.; Valdes-Garcia, A.; Avouris, P. Ultrafast graphene photodetector. *Nat. Nanotechnol.* **2009**, *4*, 839–843.

(20) Gan, X.; Shiue, R.-J.; Gao, Y.; Meric, I.; Heinz, T. F.; Shepard, K.; Hone, J.; Assefa, S.; Englund, D. Chip-integrated ultrafast graphene photodetector with high responsivity. *Nat. Photonics* **2013**, *7*, 883–887.

(21) Novoselov, K. S.; Jiang, D.; Schedin, F.; Booth, T. J.; Khotkevich, V. V; Morozov, S. V; Geim, A. K. Two-dimensional atomic crystals. *Proc. Natl. Acad. Sci. U. S. A.* **2005**, *102*, 10451–10453.

(22) Geim, A. K.; Grigorieva, I. V. Van der Waals heterostructures. *Nature* **2013**, *499*, 419–425.

(23) Lopez-Sanchez, O.; Lembke, D.; Kayci, M.; Radenovic, A.; Kis, A. Ultrasensitive photodetectors based on monolayer MoS2. *Nat. Nanotechnol.* **2013**, *8*, 497–501.

(24) Tsai, D.-S.; Liu, K.-K.; Lien, D.-H.; Tsai, M.-L.; Kang, C.-F.; Lin, C.-A.; Li, L.-J.; He, J.-H. Few-Layer MoS2 with High Broadband Photogain and Fast Optical Switching for Use in Harsh Environments. *ACS Nano* **2013**, *7*, 3905–3911.

(25) Dung-Sheng Tsai; Der-Hsien Lien; Meng-Lin Tsai; Sheng-Han Su; Kuan-Ming Chen; Jr-Jian Ke; Yueh-Chung Yu; Lain-Jong Li; Jr-Hau He. Trilayered MoS2 Metal–Semiconductor–Metal Photodetectors: Photogain and Radiation Resistance. *IEEE J. Sel. Top. Quantum Electron.* **2014**, *20*, 30–35.

(26) Zhang, W.; Huang, J.-K.; Chen, C.-H.; Chang, Y.-H.; Cheng, Y.-J.; Li, L.-J. High-Gain Phototransistors Based on a CVD MoS2 Monolayer. *Adv. Mater.* **2013**, *25*, 3456–3461.

(27) Yin, Z.; Li, H.; Li, H.; Jiang, L.; Shi, Y.; Sun, Y.; Lu, G.; Zhang, Q.; Chen, X.; Zhang, H. Single-Layer MoS2 Phototransistors. *ACS Nano* **2012**, *6*, 74–80.

(28) Kwon, J.; Hong, Y. K.; Han, G.; Omkaram, I.; Choi, W.; Kim, S.; Yoon, Y. Giant Photoamplification in Indirect-Bandgap Multilayer MoS2 Phototransistors with Local Bottom-Gate Structures. *Adv. Mater.* **2015**, *27*, 2224–2230.

(29) Wu, C.-C.; Jariwala, D.; Sangwan, V. K.; Marks, T. J.; Hersam, M. C.; Lauhon, L. J. J. Elucidating the Photoresponse of Ultrathin MoS2 Field-Effect Transistors by Scanning Photocurrent Microscopy. *Phys. Chem. Lett.* **2013**, *4*, 2508–2513.

(30) Furchi, M. M.; Polyushkin, D. K.; Pospischil, A.; Mueller, T. Mechanisms of Photoconductivity in Atomically Thin MoS2. *Nano Lett.* **2014**, *14*, 6165–6170.

(31) Lee, H. S.; Min, S.-W.; Chang, Y.-G.; Park, M. K.; Nam, T.; Kim, H.; Kim, J. H.; Ryu, S.; Im, S. MoS2 Nanosheet Phototransistors with Thickness-Modulated Optical Energy Gap. *Nano Lett.* **2012**, *12*, 3695–3700.

(32) Choi, W.; Cho, M. Y.; Konar, A.; Lee, J. H.; Cha, G.-B.; Hong, S. C.; Kim, S.; Kim, J.; Jena, D.; Joo, J.; Kim, S. High-Detectivity Multilayer MoS2 Phototransistors with Spectral Response from Ultraviolet to Infrared. *Adv. Mater.* **2012**, *24*, 5832–5836.

(33) Buscema, M.; Barkelid, M.; Zwiller, V.; van der Zant, H. S. J.; Steele, G. A.; Castellanos-Gomez, A. Large and Tunable Photothermoelectric Effect in Single-Layer MoS2. *Nano Lett.* **2013**, *13*, 358–363.

(34) Zhang, W.; Chiu, M.-H.; Chen, C.-H.; Chen, W.; Li, L.-J.; Wee, A. T. S. Role of Metal Contacts in High-Performance Phototransistors Based on WSe2 Monolayers. *ACS Nano* **2014**, *8*, 8653–8661.

(35) Abderrahmane, A.; Ko, P. J.; Thu, T. V; Ishizawa, S.; Takamura, T.; Sandhu, A. High photosensitivity few-layered MoSe2 back-gated field-effect phototransistors. *Nanotechnology* **2014**, *25*, 365202.

(36) Chang, Y.-H.; Zhang, W.; Zhu, Y.; Han, Y.; Pu, J.; Chang, J.-K.; Hsu, W.-T.; Huang, J.-K.; Hsu, C.-L.; Chiu, M.-H.; Takenobu, T.; Li, H.; Wu, C.-I.; Chang, W.-H.; Wee, A. T. S.; Li, L.-J. Monolayer MoSe2 Grown by Chemical Vapor Deposition for Fast Photodetection. *ACS Nano* **2014**, *8*, 8582–8590.

(37) Xia, J.; Huang, X.; Liu, L.-Z.; Wang, M.; Wang, L.; Huang, B.; Zhu, D.-D.; Li, J.-J.; Gu, C.-Z.; Meng, X.-M. CVD synthesis of large-area, highly crystalline MoSe2 atomic layers on diverse substrates and application to photodetectors. *Nanoscale* **2014**, *6*, 8949–8955.

(38) Huo, N.; Yang, S.; Wei, Z.; Li, S.-S.; Xia, J.-B.; Li, J. Photoresponsive and Gas Sensing Field-Effect Transistors based on Multilayer WS2 Nanoflakes. *Sci. Rep.* **2014**, *4*, 5209.

(39) Hwan Lee, S.; Lee, D.; Sik Hwang, W.; Hwang, E.; Jena, D.; Jong Yoo, W. High-performance photocurrent generation from two-dimensional WS2 field-effect transistors. *Appl. Phys. Lett.* **2014**, *104*, 193113.

(40) Perea-López, N.; Elías, A. L.; Berkdemir, A.; Castro-Beltran, A.; Gutiérrez, H. R.; Feng, S.; Lv, R.; Hayashi, T.; López-Urías, F.; Ghosh, S.; Muchharla, B.; Talapatra, S.; Terrones, H.; Terrones, M. Photosensor Device Based on Few-Layered WS2 Films. *Adv. Funct. Mater.* **2013**, *23*, 5511–5517.

(41) Buscema, M.; Groenendijk, D. J.; Blanter, S. I.; Steele, G. A.; van der Zant, H. S. J.; Castellanos-Gomez, A. Fast and Broadband Photoresponse of Few-Layer Black Phosphorus Field-Effect Transistors. *Nano Lett.* **2014**, *14*, 3347–3352.

(42) Hu, P.; Wang, L.; Yoon, M.; Zhang, J.; Feng, W.; Wang, X.; Wen, Z.; Idrobo, J. C.; Miyamoto, Y.; Geohegan, D. B.; Xiao, K. Highly Responsive Ultrathin GaS Nanosheet Photodetectors on Rigid and Flexible Substrates. *Nano Lett.* **2013**, *13*, 1649–1654.

(43) Hu, P.; Wen, Z.; Wang, L.; Tan, P.; Xiao, K. Synthesis of Few-Layer GaSe Nanosheets for High Performance Photodetectors. *ACS Nano* **2012**, *6*, 5988–5994.

(44) Lei, S.; Ge, L.; Najmaei, S.; George, A.; Kappera, R.; Lou, J.; Chhowalla, M.; Yamaguchi, H.; Gupta, G.; Vajtai, R.; Mohite, A. D.; Ajayan, P. M. Evolution of the Electronic Band Structure and Efficient Photo-Detection in Atomic Layers of InSe. *ACS Nano* **2014**, *8*, 1263–1272.

(45) Liu, F.; Shimotani, H.; Shang, H.; Kanagasekaran, T.; Zólyomi, V.; Drummond, N.; Fal'ko, V. I.; Tanigaki, K. High-Sensitivity Photodetectors Based on Multilayer GaTe Flakes. *ACS Nano* **2014**, *8*, 752–760.

(46) Su, G.; Hadjiev, V. G.; Loya, P. E.; Zhang, J.; Lei, S.; Maharjan, S.; Dong, P.; M Ajayan, P.; Lou, J.; Peng, H. Chemical Vapor Deposition of Thin Crystals of Layered Semiconductor SnS2 for Fast Photodetection Application. *Nano Lett.* **2015**, *15*, 506–513.

(47) Tamalampudi, S. R.; Lu, Y.-Y.; Kumar U, R.; Sankar, R.; Liao, C.-D.; Moorthy B, K.; Cheng, C.-H.; Chou, F. C.; Chen, Y.-T. High Performance and Bendable Few-Layered InSe Photodetectors with Broad Spectral Response. *Nano Lett.* **2014**, *14*, 2800–2806.

(48) Jacobs-Gedrim, R. B.; Shanmugam, M.; Jain, N.; Durcan, C. A.; Murphy, M. T.; Murray, T. M.; Matyi, R. J.; Moore, R. L.; Yu, B. Extraordinary Photoresponse in Two-Dimensional In2Se3 Nanosheets. *ACS Nano* **2014**, *8*, 514–521.

(49) Youngblood, N.; Chen, C.; Koester, S. J.; Li, M. Waveguide-integrated black

phosphorus photodetector with high responsivity and low dark current. *Nat. Photonics* **2015**, *9*, 247–252.

(50) Wu, J.; Koon, G. K. W.; Xiang, D.; Han, C.; Toh, C. T.; Kulkarni, E. S.; Verzhbitskiy, I.; Carvalho, A.; Rodin, A. S.; Koenig, S. P.; Eda, G.; Chen, W.; Neto, A. H. C.; Özyilmaz, B. Colossal Ultraviolet Photoresponsivity of Few-Layer Black Phosphorus. *ACS Nano* **2015**, *9*, 8070–8077.

(51) Castellanos-Gomez, A. Black Phosphorus: Narrow Gap, Wide Applications. *J. Phys. Chem. Lett.* **2015**, *6*, 4280–4291.

(52) Nathan, A.; Ahnood, A.; Cole, M. T.; Suzuki, Y.; Hiralal, P.; Bonaccorso, F.; Hasan, T.; Garcia-Gancedo, L.; Dyadyusha, A.; Haque, S.; Andrew, P.; Hofmann, S.; Moultrie, J.; Flewitt, A. J.; Ferrari, A. C.; Kelly, M. J.; Robertson, J.; Amaratunga, G. A. J.; Milne, W. I. Flexible Electronics: The Next Ubiquitous Platform. *Proc. IEEE* **2012**, *100*, 1486–1517.

(53) Akinwande, D.; Petrone, N.; Hone, J. Two-dimensional flexible nanoelectronics. *Nat. Commun.* **2014**, *5*, 5678.

(54) Chang, H.-Y.; Yang, S.; Lee, J.; Tao, L.; Hwang, W.-S.; Jena, D.; Lu, N.; Akinwande, D. High-Performance, Highly Bendable MoS2 Transistors with High-K Dielectrics for Flexible Low-Power Systems. *ACS Nano* **2013**, *7*, 5446–5452.

(55) Lee, G.-H.; Yu, Y.-J.; Cui, X.; Petrone, N.; Lee, C.-H.; Choi, M. S.; Lee, D.-Y.; Lee, C.; Yoo, W. J.; Watanabe, K.; Taniguchi, T.; Nuckolls, C.; Kim, P.; Hone, J. Flexible and Transparent MoS2 Field-Effect Transistors on Hexagonal Boron Nitride-Graphene Heterostructures. *ACS Nano* **2013**, *7*, 7931–7936.

(56) Mak, K. F.; Lee, C.; Hone, J.; Shan, J.; Heinz, T. F. Atomically Thin MoS2: A New Direct-Gap Semiconductor. *Phys. Rev. Lett.* **2010**, *105*, 136805.

(57) Bernardi, M.; Palummo, M.; Grossman, J. C. Extraordinary Sunlight Absorption and One Nanometer Thick Photovoltaics Using Two-Dimensional Monolayer Materials. *Nano Lett.* **2013**, *13*, 3664–3670.

(58) Kufer, D.; Konstantatos, G. Highly Sensitive, Encapsulated MoS2 Photodetector with Gate Controllable Gain and Speed. *Nano Lett.* **2015**, *15*, 7307–7313.

(59) Radisavljevic, B.; Radenovic, A.; Brivio, J.; Giacometti, V.; Kis, A. Single-layer MoS2 transistors. *Nat. Nanotechnol.* **2011**, *6*, 147–150.

(60) Yoon, Y.; Ganapathi, K.; Salahuddin, S. How Good Can Monolayer MoS2 Transistors Be? *Nano Lett.* **2011**, *11*, 3768–3773.

(61) Kufer, D.; Nikitskiy, I.; Lasanta, T.; Navickaite, G.; Koppens, F. H. L.; Konstantatos,

G. Hybrid 2D–0D MoS2–PbS Quantum Dot Photodetectors. *Adv. Mater.* **2015**, *27*, 176–180.

(62) Eda, G.; Maier, S. A. Two-Dimensional Crystals: Managing Light for Optoelectronics *ACS Nano* **2013**, *7*, 5660–5665.

(63) Amani, M.; Lien, D.-H.; Kiriya, D.; Xiao, J.; Azcatl, A.; Noh, J.; Madhvapathy, S. R.; Addou, R.; KC, S.; Dubey, M.; Cho, K.; Wallace, R. M.; Lee, S.-C.; He, J.-H.; Ager, J. W.; Zhang, X.; Yablonovitch, E.; Javey, A. Near-unity photoluminescence quantum yield in MoS_2. *Science (80-.).* **2015**, *350*, 1065–1068.

(64) Cheiwchanchamnangij, T.; Lambrecht, W. R. L. Quasiparticle band structure calculation of monolayer, bilayer, and bulk MoS2. *Phys. Rev. B* **2012**, *85*, 205302.

(65) Ramasubramaniam, A. Large excitonic effects in monolayers of molybdenum and tungsten dichalcogenides. *Phys. Rev. B* **2012**, *86*, 115409.

(66) Mak, K. F.; Shan, J. Photonics and optoelectronics of 2D semiconductor transition metal dichalcogenides. *Nat. Photonics* **2016**, *10*, 216–226.

(67) Wang, H.; Zhang, C.; Rana, F. Ultrafast Dynamics of Defect-Assisted Electron–Hole Recombination in Monolayer MoS2. *Nano Lett.* **2015**, *15*, 339–345.

(68) Rose, A. Recombination Processes in Insulators and Semiconductors. *Phys. Rev.* **1955**, *97*, 322–333.

(69) Liu, X.; Galfsky, T.; Sun, Z.; Xia, F.; Lin, E.; Lee, Y.-H.; Kéna-Cohen, S.; Menon, V. M. Strong light–matter coupling in two-dimensional atomic crystals. *Nat. Photonics* **2014**, *9*, 30–34.

(70) Konstantatos, G.; Badioli, M.; Gaudreau, L.; Osmond, J.; Bernechea, M.; Garcia de Arquer, F. P.; Gatti, F.; Koppens, F. H. L. Hybrid graphene–quantum dot phototransistors with ultrahigh gain. *Nat. Nanotechnol.* **2012**, *7*, 363–368.

(71) Sun, Z.; Liu, Z.; Li, J.; Tai, G.-A.; Lau, S.-P.; Yan, F. Infrared Photodetectors Based on CVD-Grown Graphene and PbS Quantum Dots with Ultrahigh Responsivity. *Adv. Mater.* **2012**, *24*, 5878–5883.

(72) Lee, Y.; Kwon, J.; Hwang, E.; Ra, C.-H.; Yoo, W. J.; Ahn, J.-H.; Park, J. H.; Cho, J. H. High-Performance Perovskite–Graphene Hybrid Photodetector. *Adv. Mater.* **2015**, *27*, 41–46.

(73) Liu, Y.; Wang, F.; Wang, X.; Wang, X.; Flahaut, E.; Liu, X.; Li, Y.; Wang, X.; Xu, Y.; Shi, Y.; Zhang, R. Planar carbon nanotube–graphene hybrid films for high-performance broadband photodetectors. *Nat. Commun.* **2015**, *6*, 8589.

(74) Zhang, W.; Chuu, C.-P.; Huang, J.-K.; Chen, C.-H.; Tsai, M.-L.; Chang, Y.-H.; Liang,

C.-T.; Chen, Y.-Z.; Chueh, Y.-L.; He, J.-H.; Chou, M.-Y.; Li, L.-J. Ultrahigh-Gain Photodetectors Based on Atomically Thin Graphene-MoS2 Heterostructures. *Sci. Rep.* **2014**, *4*, 3826.

(75) Xu, H.; Wu, J.; Feng, Q.; Mao, N.; Wang, C.; Zhang, J. High Responsivity and Gate Tunable Graphene-MoS2 Hybrid Phototransistor. *Small* **2014**, *10*, 2300–2306.

(76) Roy, K.; Padmanabhan, M.; Goswami, S.; Sai, T. P.; Ramalingam, G.; Raghavan, S.; Ghosh, A. Graphene–MoS2 hybrid structures for multifunctional photoresponsive memory devices. *Nat. Nanotechnol.* **2013**, *8*, 826–830.

(77) Kufer D., Lasanta T., Bernechea M., Koppens F., Konstantatos G. Interface Engineering in hybrid Quantum Dot – 2D phototransistors. *ACS Photonics* **2016,** *3*, 1324-1330.

(78) Hwang, D. K.; Lee, Y. T.; Lee, H. S.; Lee, Y. J.; Shokouh, S. H.; Kyhm, J.; Lee, J.; Kim, H. H.; Yoo, T.-H.; Nam, S. H.; Son, D. I.; Ju, B.-K.; Park, M.-C.; Song, J. D.; Choi, W. K.; Im, S. Ultrasensitive PbS quantum-dot-sensitized InGaZnO hybrid photoinverter for near-infrared detection and imaging with high photogain. *NPG Asia Mater.* **2016**, *8*, e233.

(79) Nomura, K.; Ohta, H.; Takagi, A.; Kamiya, T.; Hirano, M.; Hosono, H. Room-temperature fabrication of transparent flexible thin-film transistors using amorphous oxide semiconductors. *Nature* **2004**, *432*, 488–492.

(80) Choi, S.-J.; Bennett, P.; Takei, K.; Wang, C.; Lo, C. C.; Javey, A.; Bokor, J. Short-Channel Transistors Constructed with Solution-Processed Carbon Nanotubes. *ACS Nano* **2013**, *7*, 798–803.

(81) Dürkop, T.; Getty, S. A.; Cobas, E.; Fuhrer, M. S. Extraordinary Mobility in Semiconducting Carbon Nanotubes. *Nano Lett.* **2004**, *4*, 35–39.

(82) Javey, A.; Guo, J.; Wang, Q.; Lundstrom, M.; Dai, H. Ballistic carbon nanotube field-effect transistors. *Nature* **2003**, *424*, 654–657.

(83) Li, X.; Jia, Y.; Cao, A. Tailored Single-Walled Carbon Nanotube−CdS Nanoparticle Hybrids for Tunable Optoelectronic Devices. *ACS Nano* **2010**, *4*, 506–512.

(84) Liu, S.; Li, J.; Shen, Q.; Cao, Y.; Guo, X.; Zhang, G.; Feng, C.; Zhang, J.; Liu, Z.; Steigerwald, M. L.; Xu, D.; Nuckolls, C. Mirror-image photoswitching of individual single-walled carbon nanotube transistors coated with titanium dioxide. *Angew. Chem. Int. Ed. Engl.* **2009**, *48*, 4759–4762.

(85) Hu, L.; Zhao, Y.-L.; Ryu, K.; Zhou, C.; Stoddart, J. F.; Grüner, G. Light-Induced Charge Transfer in Pyrene/CdSe-SWNT Hybrids. *Adv. Mater.* **2008**, *20*, 939–946.

(86) Wang, H.; Li, F.; Kufer, D.; Yu, W.; Alarousu, E.; Ma, C.; Li, Y.; Liu, Z.; Liu, C.; Wei, N.; Chen, Y.; Wang, F.; Chen, L.; Mohammed, O. F.; Fratalocchi, A.; Konstantatos, G.; Wu, T. Achieving ultrahigh carrier mobility and photo-responsivity in solution-processed perovskite/carbon nanotubes phototransistors. arXiv:1512.03893.

(87) Lu, R.; Christianson, C.; Kirkeminde, A.; Ren, S.; Wu, J. Extraordinary Photocurrent Harvesting at Type-II Heterojunction Interfaces: Toward High Detectivity Carbon Nanotube Infrared Detectors. *Nano Lett.* **2012**, *12*, 6244–6249.

(88) Pradhan, B.; Setyowati, K.; Liu, H.; Waldeck, D. H.; Chen, J. Carbon Nanotube−Polymer Nanocomposite Infrared Sensor. *Nano Lett.* **2008**, *8*, 1142–1146.

(89) Zhou, X.; Zifer, T.; Wong, B. M.; Krafcik, K. L.; Léonard, F.; Vance, A. L. Color Detection Using Chromophore-Nanotube Hybrid Devices. *Nano Lett.* **2009**, *9*, 1028–1033.

(90) Simmons, J. M.; In, I.; Campbell, V. E.; Mark, T. J.; Léonard, F.; Gopalan, P.; Eriksson, M. A. Optically Modulated Conduction in Chromophore-Functionalized Single-Wall Carbon Nanotubes. *Phys. Rev. Lett.* **2007**, *98*, 086802.

(91) Park, S.; Kim, S. J.; Nam, J. H.; Pitner, G.; Lee, T. H.; Ayzner, A. L.; Wang, H.; Fong, S. W.; Vosgueritchian, M.; Park, Y. J.; Brongersma, M. L.; Bao, Z. Significant Enhancement of Infrared Photodetector Sensitivity Using a Semiconducting Single-Walled Carbon Nanotube/C60 Phototransistor. *Adv. Mater.* **2015**, *27*, 759–765.

(92) Appenzeller, J.; Knoch, J.; Derycke, V.; Martel, R.; Wind, S.; Avouris, P. Field-Modulated Carrier Transport in Carbon Nanotube Transistors. *Phys. Rev. Lett.* **2002**, *89*, 126801.

(93) Heinze, S.; Tersoff, J.; Martel, R.; Derycke, V.; Appenzeller, J.; Avouris, P. Carbon Nanotubes as Schottky Barrier Transistors. *Phys. Rev. Lett.* **2002**, *89*, 106801.

(94) Appenzeller, J.; Radosavljević, M.; Knoch, J.; Avouris, P. Tunneling Versus Thermionic Emission in One-Dimensional Semiconductors. *Phys. Rev. Lett.* **2004**, *92*, 048301.

(95) Knoch, J.; Zhang, M.; Appenzeller, J.; Mantl, S. Physics of ultrathin-body silicon-on-insulator Schottky-barrier field-effect transistors. *Appl. Phys. A* **2007**, *87*, 351–357.

(96) Das, S.; Chen, H.-Y.; Penumatcha, A. V.; Appenzeller, J. High Performance Multilayer MoS2 Transistors with Scandium Contacts. *Nano Lett.* **2013**, *13*, 100–105.

(97) Penumatcha, A. V; Salazar, R. B.; Appenzeller, J. Analysing black phosphorus transistors using an analytic Schottky barrier MOSFET model. *Nat. Commun.* **2015**, *6*, 8948.

(98) Ghatak, S.; Mukherjee, S.; Jain, M.; Sarma, D. D.; Ghosh, A. Microscopic origin of low frequency noise in MoS2 field-effect transistors. *APL Mater.* **2014**, *2*, 092515.

(99) Liu, W.; Kang, J.; Sarkar, D.; Khatami, Y.; Jena, D.; Banerjee, K. Role of Metal Contacts in Designing High-Performance Monolayer n-Type WSe2 Field Effect Transistors. *Nano Lett.* **2013**, *13*, 1983–1990.

(100) Cui, X.; Lee, G.-H.; Kim, Y. D.; Arefe, G.; Huang, P. Y.; Lee, C.-H.; Chenet, D. A.; Zhang, X.; Wang, L.; Ye, F.; Pizzocchero, F.; Jessen, B. S.; Watanabe, K.; Taniguchi, T.; Muller, D. A.; Low, T.; Kim, P.; Hone, J. Multi-terminal transport measurements of MoS2 using a van der Waals heterostructure device platform. *Nat. Nanotechnol.* **2015**, *10*, 534–540.

(101) Yang, L.; Majumdar, K.; Liu, H.; Du, Y.; Wu, H.; Hatzistergos, M.; Hung, P. Y.; Tieckelmann, R.; Tsai, W.; Hobbs, C.; Ye, P. D. Chloride Molecular Doping Technique on 2D Materials: WS2 and MoS2. *Nano Lett.* **2014**, *14*, 6275–6280.

(102) Kappera, R.; Voiry, D.; Yalcin, S. E.; Branch, B.; Gupta, G.; Mohite, A. D.; Chhowalla, M. Phase-engineered low-resistance contacts for ultrathin MoS2 transistors. *Nat. Mater.* **2014**, *13*, 1128–1134.

(103) Chuang, H.-J.; Chamlagain, B.; Koehler, M.; Perera, M. M.; Yan, J.; Mandrus, D.; Tománek, D.; Zhou, Z. Low-Resistance 2D/2D Ohmic Contacts: A Universal Approach to High-Performance WSe2, MoS2, and MoSe2 Transistors. *Nano Lett.* **2016**, *16*, 1896–1902.

(104) Jariwala, D.; Sangwan, V. K.; Late, D. J.; Johns, J. E.; Dravid, V. P.; Marks, T. J.; Lauhon, L. J.; Hersam, M. C. Band-like transport in high mobility unencapsulated single-layer MoS2 transistors. *Appl. Phys. Lett.* **2013**, *102*, 173107.

(105) Wu, J.; Schmidt, H.; Amara, K. K.; Xu, X.; Eda, G.; Özyilmaz, B. Large Thermoelectricity via Variable Range Hopping in Chemical Vapor Deposition Grown Single-Layer MoS2. *Nano Lett.* **2014**, *14*, 2730–2734.

(106) Qiu, H.; Xu, T.; Wang, Z.; Ren, W.; Nan, H.; Ni, Z.; Chen, Q.; Yuan, S.; Miao, F.; Song, F.; Long, G.; Shi, Y.; Sun, L.; Wang, J.; Wang, X. Hopping transport through defect-induced localized states in molybdenum disulphide. *Nat. Commun.* **2013**, *4*, 2642.

(107) Schmidt, H.; Giustiniano, F.; Eda, G. Electronic transport properties of transition metal dichalcogenide field-effect devices: surface and interface effects. *Chem. Soc. Rev.* **2015**, *44*, 7715–7736.

(108) Choi, K.; Raza, S. R. A.; Lee, H. S.; Jeon, P. J.; Pezeshki, A.; Min, S.-W.; Kim, J. S.;

Yoon, W.; Ju, S.-Y.; Lee, K.; Im, S. Trap density probing on top-gate MoS2 nanosheet field-effect transistors by photo-excited charge collection spectroscopy. *Nanoscale* **2015**, *7*, 5617–5623.

(109) Radisavljevic, B.; Kis, A. Mobility engineering and a metal–insulator transition in monolayer MoS2. *Nat. Mater.* **2013**, *12*, 815–820.

(110) Alivisatos, A. P. Perspectives on the Physical Chemistry of Semiconductor Nanocrystals. *J. Phys. Chem.* **1996**, *100*, 13226–13239.

(111) Moreels, I.; Justo, Y.; De Geyter, B.; Haustraete, K.; Martins, J. C.; Hens, Z. Size-Tunable, Bright, and Stable PbS Quantum Dots: A Surface Chemistry Study. *ACS Nano* **2011**, *5*, 2004–2012.

(112) Choi, H.; Ko, J.-H.; Kim, Y.-H.; Jeong, S. Steric-Hindrance-Driven Shape Transition in PbS Quantum Dots: Understanding Size-Dependent Stability. *J. Am. Chem. Soc.* **2013**, *135*, 5278–5281.

(113) Hines, M. A.; Scholes, G. D. Colloidal PbS Nanocrystals with Size-Tunable Near-Infrared Emission: Observation of Post-Synthesis Self-Narrowing of the Particle Size Distribution. *Adv. Mater.* **2003**, *15*, 1844–1849.

(114) Choi, J.J.; Luria, J; Hyun, B.R.; Bartnik, A. C.; Sun, L.; Lim, Y.F.; Marohn, J. A.; Wise, F. W.; Hanrath T. Photogenerated Exciton Dissociation in Highly Coupled Lead Salt Nanocrystal Assemblies. *Nano Lett.* **2010**, 10, 1805–1811.

(115) Zhitomirsky, D.; Voznyy, O.; Levina, L.; Hoogland, S.; Kemp, K. W.; Ip, A. H.; Thon, S. M.; Sargent, E. H. Engineering colloidal quantum dot solids within and beyond the mobility-invariant regime. *Nat. Commun.* **2014**, *5*, 3803.

(116) Stavrinadis, A.; Konstantatos, G. Strategies for the Controlled Electronic Doping of Colloidal Quantum Dot Solids. *Chemphyschem* **2016**, *17*, 632–644.

(117) Bao, J.; Bawendi, M. G. A colloidal quantum dot spectrometer. *Nature* **2015**, *523*, 67–70.

(118) Kim, T.-H.; Cho, K.-S.; Lee, E. K.; Lee, S. J.; Chae, J.; Kim, J. W.; Kim, D. H.; Kwon, J.-Y.; Amaratunga, G.; Lee, S. Y.; Choi, B. L.; Kuk, Y.; Kim, J. M.; Kim, K. Full-colour quantum dot displays fabricated by transfer printing. *Nat. Photonics* **2011**, *5*, 176–182.

(119) Choi, M. K.; Yang, J.; Kang, K.; Kim, D. C.; Choi, C.; Park, C.; Kim, S. J.; Chae, S. I.; Kim, T.-H.; Kim, J. H.; Hyeon, T.; Kim, D.-H. Wearable red–green–blue quantum dot light-emitting diode array using high-resolution intaglio transfer printing. *Nat. Commun.* **2015**, *6*, 7149.

(120) Liu, H.; Li, M.; Voznyy, O.; Hu, L.; Fu, Q.; Zhou, D.; Xia, Z.; Sargent, E. H.; Tang, J. Physically Flexible, Rapid-Response Gas Sensor Based on Colloidal Quantum Dot Solids. *Adv. Mater.* **2014**, *26*, 2718–2724, 2617.

(121) Snaith, H. J. Perovskites: The Emergence of a New Era for Low-Cost, High-Efficiency Solar Cells. *J. Phys. Chem. Lett.* **2013**, *4*, 3623–3630.

(122) Xing, G.; Mathews, N.; Lim, S. S.; Yantara, N.; Liu, X.; Sabba, D.; Grätzel, M.; Mhaisalkar, S.; Sum, T. C. Low-temperature solution-processed wavelength-tunable perovskites for lasing. *Nat. Mater.* **2014**, *13*, 476–480.

(123) Stranks, S. D.; Eperon, G. E.; Grancini, G.; Menelaou, C.; Alcocer, M. J. P.; Leijtens, T.; Herz, L. M.; Petrozza, A.; Snaith, H. J. Electron-Hole Diffusion Lengths Exceeding 1 Micrometer in an Organometal Trihalide Perovskite Absorber. *Science* **2013**, *342*, 341–344.

(124) Shi, D.; Adinolfi, V.; Comin, R.; Yuan, M.; Alarousu, E.; Buin, A.; Chen, Y.; Hoogland, S.; Rothenberger, A.; Katsiev, K.; Losovyj, Y.; Zhang, X.; Dowben, P. A.; Mohammed, O. F.; Sargent, E. H.; Bakr, O. M. Low trap-state density and long carrier diffusion in organolead trihalide perovskite single crystals. *Science (80-.).* **2015**, *347*, 519–522.

(125) Guo, Y.; Liu, C.; Tanaka, H.; Nakamura, E. Air-Stable and Solution-Processable Perovskite Photodetectors for Solar-Blind UV and Visible Light. *J. Phys. Chem. Lett.* **2015**, *6*, 535–539.

(126) Saidaminov, M. I.; Adinolfi, V.; Comin, R.; Abdelhady, A. L.; Peng, W.; Dursun, I.; Yuan, M.; Hoogland, S.; Sargent, E. H.; Bakr, O. M. Planar-integrated single-crystalline perovskite photodetectors. *Nat. Commun.* **2015**, *6*, 8724.

(127) Dou, L.; Yang, Y. M.; You, J.; Hong, Z.; Chang, W.-H.; Li, G.; Yang, Y. Solution-processed hybrid perovskite photodetectors with high detectivity. *Nat. Commun.* **2014**, *5*, 5404.

(128) Fang, Y.; Huang, J. Resolving Weak Light of Sub-picowatt per Square Centimeter by Hybrid Perovskite Photodetectors Enabled by Noise Reduction. *Adv. Mater.* **2015**, *27*, 2804–2810.

(129) Li, F.; Ma, C.; Wang, H.; Hu, W.; Yu, W.; Sheikh, A. D.; Wu, T. Ambipolar solution-processed hybrid perovskite phototransistors. *Nat. Commun.* **2015**, *6*, 8238.

(130) Fang, Y.; Dong, Q.; Shao, Y.; Yuan, Y.; Huang, J. Highly narrowband perovskite single-crystal photodetectors enabled by surface-charge recombination. *Nat. Photonics* **2015**, *9*, 679–686.

(131) Schwierz, F. Graphene transistors. *Nat. Nanotechnol.* **2010**, *5*, 487–496.

(132) Lembke, D.; Bertolazzi, S.; Kis, A. Single-Layer MoS2 Electronics. *Acc. Chem. Res.* **2015**, *48*, 100–110.

(133) Fiori, G.; Bonaccorso, F.; Iannaccone, G.; Palacios, T.; Neumaier, D.; Seabaugh, A.; Banerjee, S. K.; Colombo, L. Electronics based on two-dimensional materials. *Nat. Nanotechnol.* **2014**, *9*, 768–779.

(134) Li, L.; Yu, Y.; Ye, G. J.; Ge, Q.; Ou, X.; Wu, H.; Feng, D.; Chen, X. H.; Zhang, Y. Black phosphorus field-effect transistors. *Nat. Nanotechnol.* **2014**, *9*, 372–377.

(135) Tada, A.; Geng, Y.; Wei, Q.; Hashimoto, K.; Tajima, K. Tailoring organic heterojunction interfaces in bilayer polymer photovoltaic devices. *Nat. Mater.* **2011**, *10*, 450–455.

(136) He, Z.; Zhong, C.; Huang, X.; Wong, W.-Y.; Wu, H.; Chen, L.; Su, S.; Cao, Y. Simultaneous Enhancement of Open-Circuit Voltage, Short-Circuit Current Density, and Fill Factor in Polymer Solar Cells. *Adv. Mater.* **2011**, *23*, 4636–4643.

(137) Barnea-Nehoshtan, L.; Nayak, P. K.; Shu, A.; Bendikov, T.; Kahn, A.; Cahen, D. Enhancing the Tunability of the Open-Circuit Voltage of Hybrid Photovoltaics with Mixed Molecular Monolayers. *ACS Appl. Mater. Interfaces* **2014**, *6*, 2317–2324.

(138) Chuang, C.-H. M.; Brown, P. R.; Bulović, V.; Bawendi, M. G. Improved performance and stability in quantum dot solar cells through band alignment engineering. *Nat. Mater.* **2014**, *13*, 796–801.

(139) Nikitskiy I., Goossens S., Kufer D.,Lasanta T., Navickaite G., Koppens F., K. G. Integrating an electrically active colloidal quantum dot photodiode with a graphene phototransistor. *Nat. Commun.* **2016,** *7*, 11954.

(140) Keuleyan, S.; Lhuillier, E.; Brajuskovic, V.; Guyot-Sionnest, P. Mid-infrared HgTe colloidal quantum dot photodetectors. *Nat. Photonics* **2011**, *5*, 489–493.

(141) Adinolfi, V.; Kramer, I. J.; Labelle, A. J.; Sutherland, B. R.; Hoogland, S.; Sargent, E. H. Photojunction Field-Effect Transistor Based on a Colloidal Quantum Dot Absorber Channel Layer. *ACS Nano* **2015**, *9*, 356–362.

(142) Ma, C.; Shi, Y.; Hu, W.; Chiu, M.-H.; Liu, Z.; Bera, A.; Li, F.; Wang, H.; Li, L.-J.; Wu, T. Heterostructured WS2/CH3NH3PbI3 Photoconductors with Suppressed Dark Current and Enhanced Photodetectivity. *Adv. Mater.* **2016**, 28, 3683–3689.

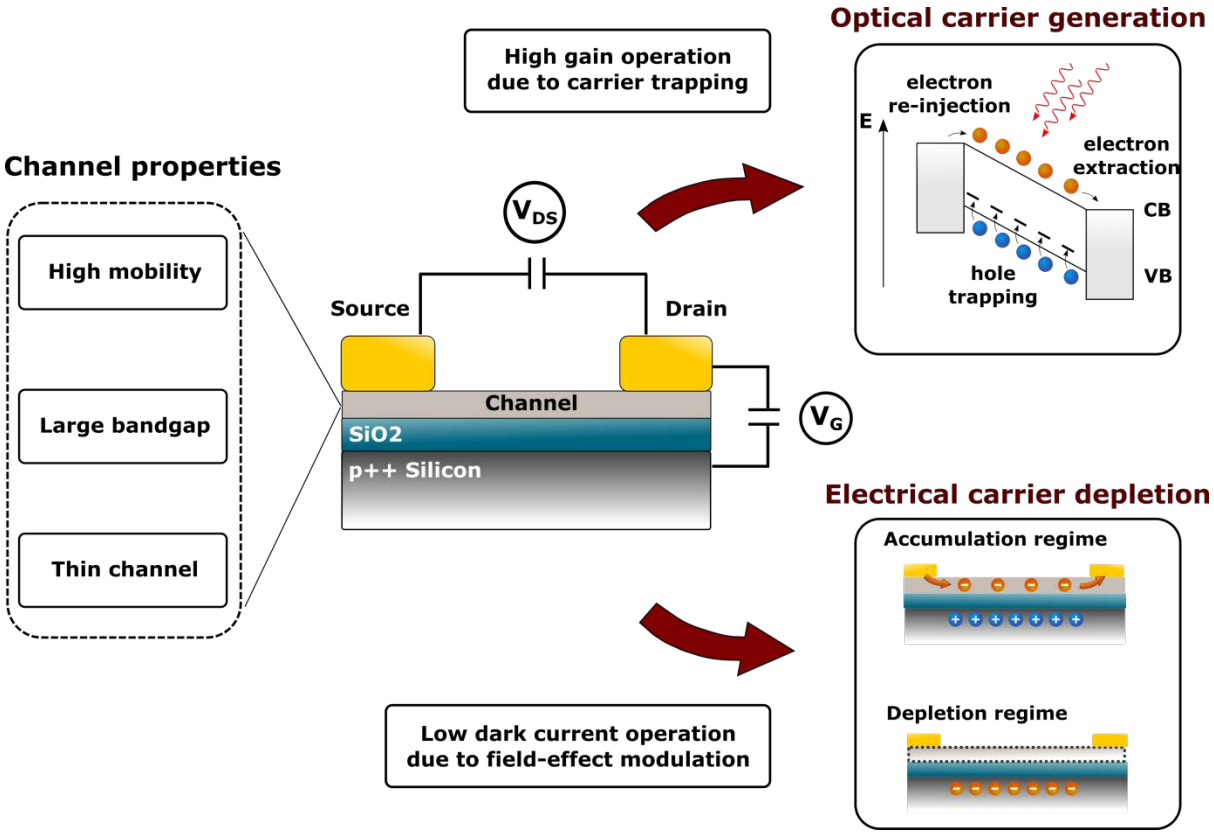

Figure 1. Device design and functionality. The device configuration of a photo-FET is similar to lateral photoconductors with metal-semiconductor-metal architecture. The two metal electrodes in contact with the channel material form the source and drain electrodes, where the bias V_{DS} is applied. The gate electrode, here a highly doped silicon slab, is electrically isolated from the semiconductor channel by a thin dielectric film (e.g. SiO_2). An applied gate voltage V_{GS} can be used to control electronically the dark conductivity by field-effect modulation and favourably switch off the dark current by operating the device in the depletion regime (bottom right box). The incident light enables the channel conductance of the device and can profit from a photoconductive gain mechanism as in photoconductors (top right box). For high performance photo-FETs, the channel material possesses ideally high carrier mobility for high gain-bandwidth products, a moderately large and direct bandgap for efficient field-effect modulation and optical absorption, and a thin profile for full depletion and operation at ultralow dark currents (left box).

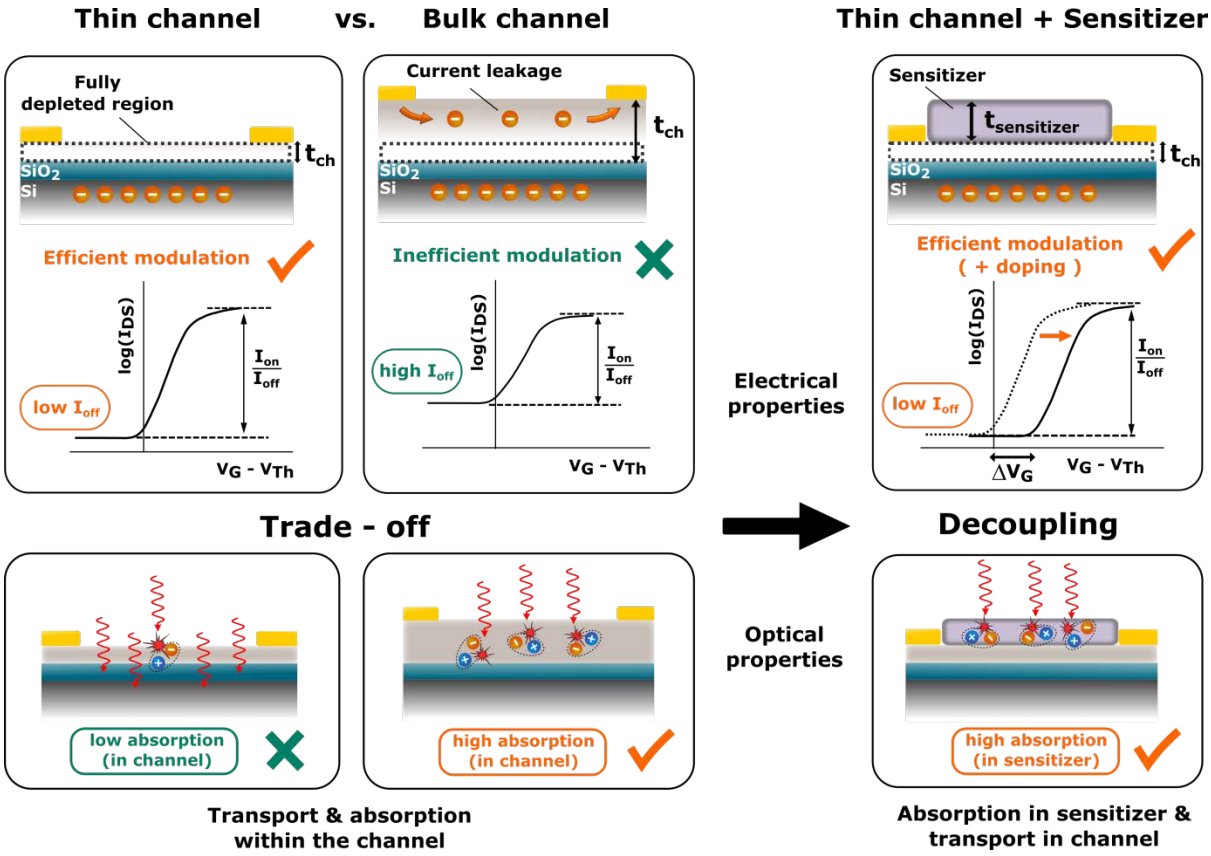

Figure 2. Transport vs. absorption dilemma. The two left columns present the typical trade-off met for 2D-based photo-FETs consisting of a thin and a thick channel. In the case of a thin channel, the thickness is typically in the range of a few nanometers. 2D-materials benefit from their atomically thin profile which allows efficient field-effect modulation leading to high on/off ratios. The channel can be fully depleted and operated at extremely low off-state currents under dark (upper box). While the conditions for electronic transport are ideal, the absorption of photons in nanometer-scale channel thickness is rather inefficient and limits the detector response (lower box). In case of a thicker channel, with thickness of around 100-200nm, the transport and absorption behaves viceversa. The field-effect depletes only the region at the oxide-interface and significant leakage through the upper part of the channel remains. This yields in reduced on/off ratio and considerably higher off-state currents. However, here the absorption profits from longer optical path throught the semiconductor bulk. The right column depicts a solution to this dilemma by decoupling the the electronic transport from the optical absorption. Therefore a thin 2D channel is used for full depletion and ideal transport conditions with low off-state current and a sensitizing absorber is deposited on top of the channel for efficient light absorption. The thickness of the decorating sensitizer can be in dimensions similar to the bulk case and thereby transport and absorption properties are similarly optimized.

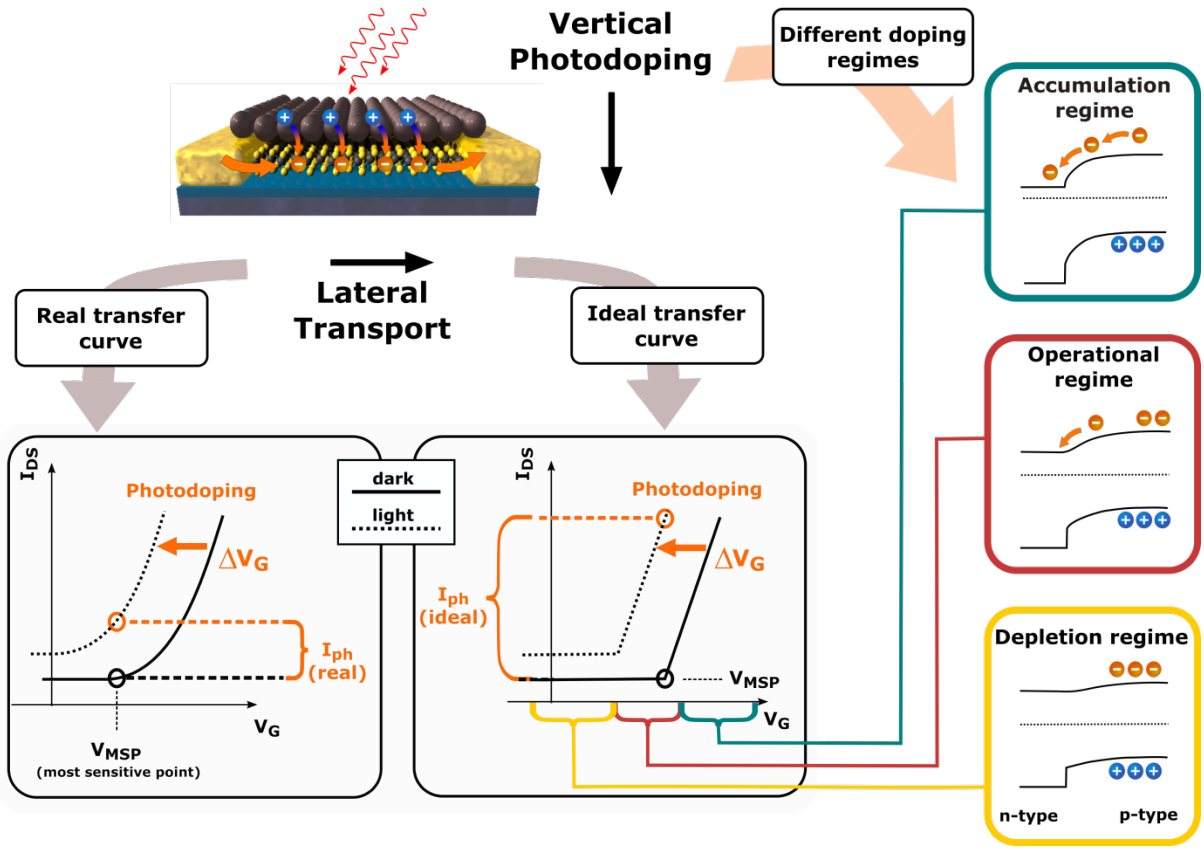

Figure 3. Operation principle, ideal transport and photodoping conditions. The device schematic shows the light sensing process of a sensitized photo-FET using the example of a n-type semiconductor channel and a p-type QD sensitizer. After the absorption process, a fast recombination of photogenerated carriers is prevented due to spatial separation of carriers in the heterojunction. The p-n-junction between the oppositely doped semiconductors leads to a vertical photodoping effect. As long as the holes maintain trapped within the sensitizer, the injected electrons recirculate the channel and generate gain. The photoconductive gain, the dark current, and the quantum efficiency of the hybrid photo-FET depend strongly on the gate voltage operation, as illustrated by the comparison of a real and an ideal transfer curve (bottom black boxes) and the band alignment in the different operational regimes (right coloured boxes). The most sensitive point (V_{MSP}) for gain and dark current is ideally located as close as possible to the current onset of the transfer characteristic. A fast switching behaviour between the off- and on-state, as shown in the ideal case, leads to optimized operation of the photo-FET with low dark currents and high photoconductive gain. The ideal photodoping conditions are given in the accumulation regime, where the strongest band bending occurs and the largest depletion region will be formed at the heterojunction. The best performance of the sensitized

photo-FET lies in the operational regime, where dark current, gain, and quantum efficiency are optimized.